

A new shape function and some specific wormhole solutions in braneworld scenario

Bikram Ghosh* and Saugata Mitra†

Department of Mathematics, Ramakrishna Mission Vidyamandira, Howrah-711202, West Bengal, India

Considering a energy density of the form $\rho = q \left(\frac{r}{r_0} \right)^{-n}$ (where q is an arbitrary positive constant with dimension of energy density and $n > 0$), a shape function is obtained by using field equations of braneworld gravity theory in this paper. Under isotropic scenario wormhole solutions are obtained considering six different redshift functions along with the obtained new shape function. For anisotropic case wormhole solutions are obtained under the consideration of five different shape functions along with the redshift function $\phi = \beta \ln \left(\frac{r}{r_0} \right)$, where β is an arbitrary constant. In each case all the energy conditions are examined and it is found that for some cases all energy conditions are satisfied in the vicinity of the wormhole throat and for the rest cases all energy conditions are satisfied except strong energy condition.

I. INTRODUCTION

In the context of string theory[1]–[2], the brane (*i.e.*, the observed four dimensional world) is considered as a domain wall in the five dimensional space-time. Geometrically, brane[3]–[4] is considered as a four dimensional hypersurface embedded in a five dimensional bulk (for a review see[5]–[6]). In Randall-Sundrum type-II[4] brane model, our universe (*i.e.*, 3 brane) is embedded in a five-dimensional bulk with extra dimension extending to infinity in either side of the brane. In this model all standard model fields are confined to the brane while gravity can propagate in the surrounding bulk. Starting from the five-dimensional Einstein field equations in the bulk and using Gauss and Codazzi equations Shiromizu et al.[7] derived the modified four-dimensional Einstein equations on the brane. The above modified Einstein field equations has two extra terms in the r.h.s– one correction term is quadratic in the energy-momentum tensor on the brane and is termed as local bulk effect while the non-local bulk effect is the electric part of the 5D Weyl tensor. Hence the effective Einstein equations on the brane can be written as [8]–[10]

$$G_{\mu\nu} = -\Lambda g_{\mu\nu} + k^2(T_{\mu\nu} + \frac{6}{\lambda}P_{\mu\nu}) - \xi_{\mu\nu}, \quad (1)$$

where the terms on the r.h.s of the above modified Einstein equation are the followings: $\Lambda = \frac{1}{2}(\Lambda_5 + k^2\lambda)$, $k^2 = \frac{\lambda k_5^2}{6}$,

$$P_{\mu\nu} = \frac{1}{8} \left[\frac{2}{3}TT_{\mu\nu} - 2T_{\mu\psi}T_{\nu}^{\psi} + g_{\mu\nu} \left\{ T_{\psi\tau}T^{\psi\tau} - \frac{1}{3}T^2 \right\} \right], \quad (2)$$

and $\xi_{\mu\nu} = \delta_{\mu}^A \delta_{\nu}^C W_{ABCD} \eta^B \eta^D$. Here k^2 and k_5^2 are gravitational coupling constants on brane and bulk respectively, Λ and Λ_5 are the cosmological constants on the brane and bulk respectively, λ is the brane tension, $T_{\mu\nu}$ is the energy momentum tensor for the matter on the brane (with $T = T_{\mu\nu}g^{\mu\nu}$ is the trace of the energy momentum tensor), $P_{\mu\nu}$ is the local correction term, $\xi_{\mu\nu}$ is the (trace less *i.e.*, $\xi_{\mu}^{\mu} = 0$) non-local bulk effect(which is the projection of the 5D dimensional Weyl tensor W_{ABCD}) and η^a is the unit normal to the brane.

Wormhole is a hypothetical geometric structure in space-time [11]–[13]. It can be considered as tunnels in the space-time topology. In fact this topological structure connects two distant parts of a single universe or even of different universes. The wormhole geometry is characterized by the solution of the Einstein equations with exotic matter (that violates the null energy condition) at least in the vicinity of the wormhole throat[14]–[16]. In spherically symmetric space-time, traversable wormhole is most interesting and physically viable and such type of wormhole was initiated by the pioneering work of Morris and Throne[17]–[18]. The restriction in the geometry of the space-time due to the traversability nature of the wormhole is that the redshift function should not have any horizon or it is desirable to have a given asymptotic form for both the redshift and shape function. Usually, in the literature wormhole solutions are constructed knowing a priori the desired form of the redshift function and the shape function and Einstein field equations determine the matter part for the wormhole geometry.

Braneworld gravity[19] is an important model of the universe in modified gravity theory and obtaining wormhole solutions in this gravity is attracted to researchers[20]–[23], where wormhole solutions are obtained under different

* bikramghosh13@gmail.com

† saugatamitra20@gmail.com

considerations. In [8], wormhole solutions are obtained by equating R with zero. Inflating wormhole solutions are obtained in [24]. In the literature there are many examples of wormhole solutions where null energy condition is satisfied [25]-[28].

In this paper, a new shape function is found by considering a particular form of energy density and the main motivation is to examine whether all energy conditions are satisfied or not in the wormhole solutions which are obtained by considering isotropic fluid and using the new shape function along with the following redshift functions: $\phi(r) = \text{constant}$; $\phi(r) = \beta \ln\left(\frac{r}{r_0}\right)$, β is a arbitrary constant; $\phi(r) = \frac{1}{r}$; $\phi(r) = \ln\frac{\sqrt{\gamma^2+r^2}}{r}$, γ is a arbitrary constant; $\phi(r) = e^{-\frac{r_0}{r}}$; $\phi(r) = e^{-\frac{r_0}{r} - \frac{r_0^2}{r^2}}$ [29]-[30]. Other wormhole solutions for anisotropic fluid using shape functions: $b(r) = \frac{r_0^n}{r^{n-1}}$, ($n > 0$); $b(r) = \frac{r}{1+\ln(1+r-r_0)}$, ($0 < r_0 < 1$); $b(r) = \frac{r}{1+r-r_0}$, ($0 < r_0 < 1$); $b(r) = r_0 \left\{ 1 + \gamma^2 \left(1 - \frac{r_0}{r} \right) \right\}$, ($\gamma^2 \in (0, 1)$) [9] and $b(r) = r e^{\frac{2\sigma}{\delta}(r^\delta - r_0^\delta)}$ ($\sigma < 0$ and $\delta > 0$) [29]-[30] and redshift function $\phi(r) = \beta \ln\left(\frac{r}{r_0}\right)$ are obtained and energy conditions are also examined in this cases.

The paper is arranged as follows : in section II, the necessary field equations on Brane-world are discussed. In section III energy conditions of wormholes are mentioned. A wormhole shape function is obtained in section IV. Energy conditions are examined in section V for isotropic fluid. For anisotropic fluid wormhole solutions are obtained, energy conditions are examined in section VI. Lastly, we discuss our overall observations in section VII.

II. FIELD EQUATIONS ON THE BRANE

The space-time metric representing a spherically symmetric and static wormhole is given by [17]

$$ds^2 = -e^{2\phi(r)} dt^2 + \frac{dr^2}{1 - \frac{b(r)}{r}} + r^2(d\theta^2 + \sin^2\theta d\phi^2), \quad (3)$$

where $\phi(r)$ and $b(r)$ are arbitrary function of radial co-ordinate ‘ r ’, termed as redshift function and shape function respectively. The former is related to gravitational redshift, while the latter determines the shape of the wormhole. The event horizon should be absent for traversable wormhole, for which we require $e^{2\phi(r)} \neq 0$ i.e., $\phi(r)$ should be finite everywhere. Now for the existence of wormhole, the shape function $b(r)$ is restricted as follows (i) $b(r_0) = r_0$ (r_0 is the location of the throat), (ii) $\frac{b(r)}{r} < 1$ for $r > r_0$, (iii) $\frac{b(r)}{r} \rightarrow 0$ and $\phi(r) \rightarrow \phi_0$ (constant) as $r \rightarrow \infty$ (asymptotically flatness property [17]-[18]), (iv) $\frac{b-b'r}{2b^2} > 0$ is the condition for flare-out [17].

The field equation on the brane can take the form

$$G_{\mu\nu} = 8\pi T_{\mu\nu}^{\text{eff}}, \quad (4)$$

with the total effective stress-energy tensor,

$$T_{\mu\nu}^{\text{eff}} = T_{\mu\nu} - \frac{1}{8\pi} \xi_{\mu\nu} + \frac{6}{\lambda} P_{\mu\nu} \quad \text{with } k^2 = 8\pi. \quad (5)$$

For simplicity we have considered $\Lambda = 0$ on the brane and hence Einstein tensor components (with respect to an orthonormal reference frame) for the metric (3) can be written as

$$G_{tt} = \frac{b'}{r^2}, \quad (6)$$

$$G_{rr} = 2 \left(1 - \frac{1}{r} \right) \frac{\phi'}{r} - \frac{b}{r^3}, \quad (7)$$

$$G_{\theta\theta} = G_{\phi\phi} = \left(1 - \frac{b}{r} \right) \left[\phi'' + (\phi')^2 + \frac{\phi'}{r} - \frac{b'r - b}{2r^2(r - b)} - \frac{b'r - b}{2r(r - b)} \phi' \right], \quad (8)$$

where the prime denotes the derivative with respect to the radial coordinate ‘ r ’. From (1), the traceless property of the projected 5-dimensional Weyl-tensor gives [10]

$$R = -k^2 \left\{ T + \frac{3}{2\lambda} \left(T_{\psi\tau} T^{\psi\tau} - \frac{1}{3} T^2 \right) \right\} \quad (9)$$

i.e.,

$$R = -k^2 \left[(-\rho + p_r + 2p_t) + \frac{3}{2\lambda} \left\{ \rho^2 + p_r^2 + 2p_t^2 - \frac{1}{3} \left(-\rho + p_r + 2p_t \right)^2 \right\} \right]. \quad (10)$$

Also from the definition of Ricci scalar (R) [33] we get,

$$R = -2 \left(1 - \frac{b}{r} \right) \left[\phi'' + (\phi')^2 - \frac{b'}{r(r-b)} - \frac{b'r + 3b - 4r}{2r(r-b)} \phi' \right] \quad (11)$$

and the result becomes $R|_{r=r_0} = \frac{2b'_0}{r_0^3} + \frac{(b'_0-1)\phi'_0}{r_0^3}$ at the throat.

III. ENERGY CONDITIONS

The null energy condition (NEC), weak energy condition (WEC), strong energy condition (SEC) and dominant energy conditions (DEC) are considered main energy conditions in the background of brane-world gravity. These will be investigated by the following inequalities depending on energy momentum tensor characterize the energy conditions as follows [31]-[33]:

$$(I) \quad \text{NEC} : \rho + p_r \geq 0, \rho + p_t \geq 0 \quad (12)$$

$$(II) \quad \text{WEC} : \rho \geq 0, \rho + p_r \geq 0, \rho + p_t \geq 0 \quad (13)$$

$$(III) \quad \text{SEC} : \rho + p_r \geq 0, \rho + p_t \geq 0, \rho + p_r + 2p_t \geq 0 \quad (14)$$

$$(IV) \quad \text{DEC} : \rho \geq 0, \rho - |p_r| \geq 0, \rho - |p_t| \geq 0. \quad (15)$$

For the isotropic fluid with radial pressure p , the above set becomes:

$$(I) \quad \text{NEC} : \rho + p \geq 0 \quad (16)$$

$$(II) \quad \text{WEC} : \rho \geq 0, \rho + p \geq 0 \quad (17)$$

$$(III) \quad \text{SEC} : \rho + p \geq 0, \rho + 3p \geq 0 \quad (18)$$

$$(IV) \quad \text{DEC} : \rho \geq 0, \rho - |p| \geq 0. \quad (19)$$

IV. OBTAINING SHAPE FUNCTION

For an isotropic fluid on the brane, the energy momentum tensor can be written as $T_\nu^\mu = \text{diag}(-\rho, p, p, p)$ [10] where ρ is energy density, p is isotropic radial pressure of the fluid. As a result, the nonlocal bulk effects contribute in the form an effective anisotropic fluid as

$$\xi_\nu^\mu = \text{diag}[-\epsilon(r), \sigma_r(r), \sigma_t(r), \sigma_t(r)], \quad (20)$$

and the traceless property of $\xi_{\mu\nu}$ gives

$$-\epsilon + \sigma_r + 2\sigma_t = 0. \quad (21)$$

Now using equations (4) and (5) we get the effective field equations from (6)–(8) as [9]:

$$\frac{b'}{r^2} = \rho \left(1 + \frac{\rho}{2\lambda} \right) - \frac{\epsilon}{8\pi}, \quad (22)$$

$$\frac{2}{r} \left(1 - \frac{b}{r} \right) \phi' - \frac{b}{r^3} = p \left(1 + \frac{\rho}{\lambda} \right) + \frac{\rho^2}{2\lambda} - \frac{\sigma_r}{8\pi}, \quad (23)$$

$$\left(1 - \frac{b}{r} \right) \left[\phi'' + \phi' \left(\phi' + \frac{1}{r} \right) \right] - \frac{b'r - b}{2r^2} \left(\phi' + \frac{1}{r} \right) = p \left(1 + \frac{\rho}{\lambda} \right) + \frac{\rho^2}{2\lambda} - \frac{\sigma_t}{8\pi}. \quad (24)$$

It is seen that in many wormhole theory literature the energy density takes the form $\rho = kr^{-s}$ where k is a arbitrary positive constant, $s = 1.5$ in [33] and $s = 1.75$ in [34]. So let us take the form $\rho = q \left(\frac{r}{r_0} \right)^{-n}$ for $n > 0$ (where q will take care about the dimension of energy density) and try to find shape function in this scenario.

Let us consider $\epsilon = 0$. Then for the above energy density form $\rho = q \left(\frac{r}{r_0}\right)^{-n}$ for $n > 0$, the equation (22) gives

$$b' = qr_0^n r^{2-n} + \frac{q^2 r_0^{2n}}{2\lambda} r^{2-2n}. \quad (25)$$

$$\therefore b = \frac{qr_0^n}{3-n} r^{3-n} + \frac{q^2 r_0^{2n}}{2(3-2n)\lambda} r^{3-2n} + A \text{ (where } A \text{ is an arbitrary constant)}. \quad (26)$$

To be a shape function b must obey the following properties:

$$b(r_0) = r_0, \quad (27)$$

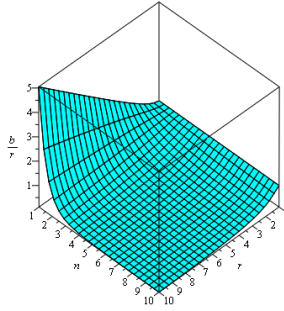
$$\frac{b}{r} \leq 1, \quad (28)$$

$$\frac{b - b'r}{b^2} > 0. \quad (29)$$

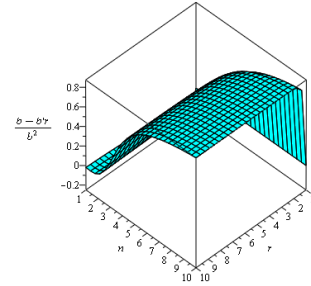
Using (27), equation (26) reduces to

$$b(r) = \frac{qr_0^n}{3-n} r^{3-n} + \frac{q^2 r_0^{2n}}{2(3-2n)\lambda} r^{3-2n} + r_0 - \frac{qr_0^3}{3-n} - \frac{q^2 r_0^3}{2(3-2n)\lambda}. \quad (30)$$

The figure(1) shows that $b(r)$ is satisfying the other require conditions to be a shape function of a wormhole for $n \in (3, 10)$ (a particular scenario is shown in figure2).

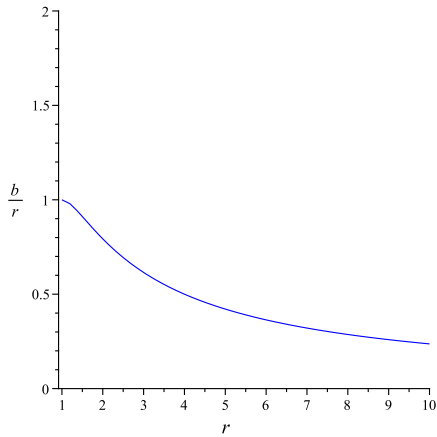


1(A)

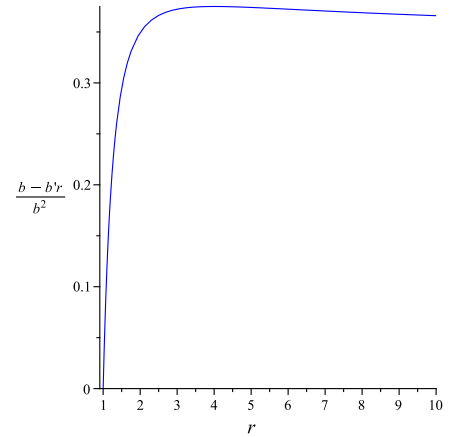


1(B)

FIG. 1: Behavior of $\frac{b(r)}{r}$ (1(A)) and $\frac{b-b'r}{b^2}$ (1(B)) with radial co-ordinate 'r' and parameter n have been plotted for obtained shape function(30) when $1 \leq n \leq 10$ and r ranges from r_0 to 10, $\lambda = 10^4$, $q = 1$ and $r_0 = 1$.



2(A)



2(B)

FIG. 2: Behavior of $\frac{b(r)}{r}$ (2(A)) and $\frac{b-b'r}{b^2}$ (2(B)) have been plotted for obtained shape function(30) against r when $n = 3.5$, $\lambda = 10^4$, $q = 1$ and $r_0 = 1$.

V. VALIDATION OF ENERGY CONDITION OF WORMHOLE SOLUTIONS CORRESPONDS TO OBTAINED SHAPE FUNCTION FOR ISOTROPIC FLUID

Now by equation (22) expression of b (30) is obtained considering $\rho = q \left(\frac{r}{r_0} \right)^{-n}$ for $n > 0$. Also equation (22) can be written as

$$b' = \frac{\rho^2 r^2}{2\lambda} + \rho r^2 \quad \text{with } b(r_0) = r_0. \quad (31)$$

The above equation(31) gives a unique solution for $b(r)$ in a neighbourhood of r_0 . So if we take $\epsilon = 0$, then we will get the same ρ for this shape function $b(r)$. For $\epsilon = 0$, equation (21) gives

$$\sigma_r = -2\sigma_t. \quad (32)$$

Using equation (32), equation (23) and (24) reduce to the form

$$A_1 p - 2B_1 \sigma_t = C_1, \quad (33)$$

$$A_1 p + B_1 \sigma_t = C_2; \quad (34)$$

$$\text{where } A_1 = 1 + \frac{\rho}{\lambda}; \quad B_1 = \frac{-1}{8\pi};$$

$$C_1 = \frac{2}{r} \left(1 - \frac{b}{r} \right) \phi' - \frac{b}{r^3} - \frac{\rho^2}{2\lambda};$$

$$C_2 = \left(1 - \frac{b}{r} \right) \left[\phi'' + \phi' \left(\phi' + \frac{1}{r} \right) \right] - \frac{b'r - b}{2r^2} \left(\phi' + \frac{1}{r} \right) - \frac{\rho^2}{2\lambda}.$$

Solving the above set of equations (33) and (34) we get,

$$p = \frac{2C_2 + C_1}{3A_1}; \quad (35)$$

$$\sigma_t = \frac{C_2 - C_1}{3B_1}. \quad (36)$$

The shape function(30) is obtained from the field equation (22) which is independent of redshift function. Now choosing different redshift functions (which are mentioned in section-I), the validation of energy conditions are examined and they are shown in the figures (3)–(9).

VI. WORMHOLE SOLUTIONS FROM FIELD EQUATIONS FOR ANISOTROPIC FLUID

We assume the relation $p_r = \alpha p_t$ ($\alpha \neq 1$) and consider a equation of state $p_t = \omega \rho$ *i.e.*, $p_r = \alpha \omega \rho$. Now we will find the wormhole solution from the above field equations (6)-(8). Using above equation of state in (10) we obtain ,

$$R = -k^2 \left[(-1 + \alpha\omega + 2\omega)\rho + \frac{\rho^2}{\lambda} (1 + \alpha^2\omega^2 + \omega^2 + \alpha\omega + 2\omega - 2\alpha\omega^2) \right] \quad (37)$$

i.e.,

$$\frac{1 + \alpha^2\omega^2 + \omega^2 + \alpha\omega + 2\omega - 2\alpha\omega^2}{\lambda} \rho^2 + (-1 + \alpha\omega + 2\omega)\rho + \frac{1}{8\pi} R = 0. \quad (38)$$

After solving the equation(38), we get

$$\rho(R) = \frac{-B \pm \sqrt{B^2 - 4AC}}{2A}, \quad \text{where } \begin{cases} A = \frac{1 + \alpha^2\omega^2 + \omega^2 + \alpha\omega + 2\omega - 2\alpha\omega^2}{\lambda} \\ B = (-1 + \alpha\omega + 2\omega) \\ C = \frac{1}{8\pi} R \end{cases}. \quad (39)$$

Consequently we have p_r and p_t (in terms of ρ). Thus from the value of R , the expression of ρ , p_r and p_t can be computed. In this section wormhole solutions will be investigated with five different shape functions considering the redshift function $\phi(r) = \beta \ln\left(\frac{r}{r_0}\right)$, where β is an arbitrary constant:

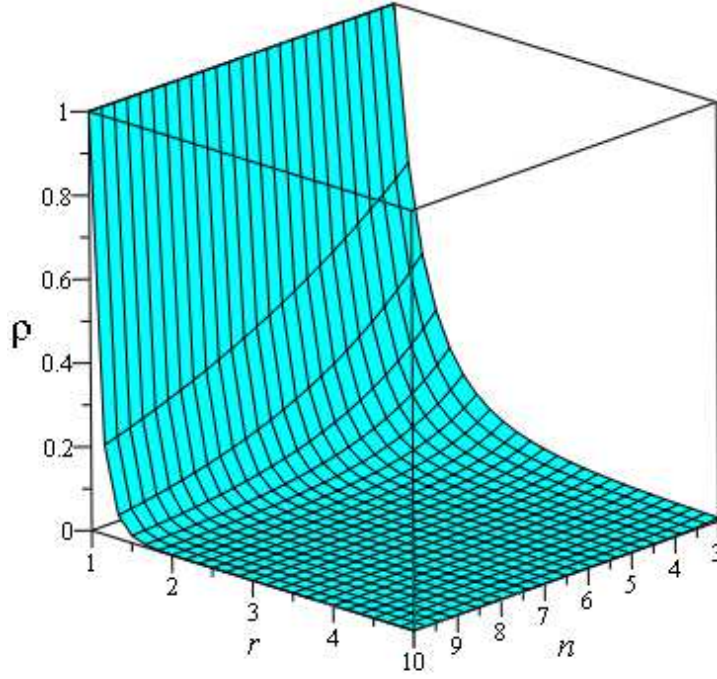
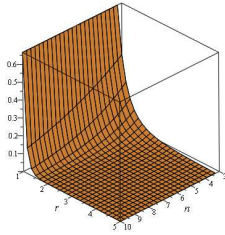
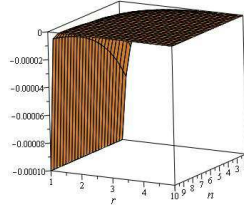


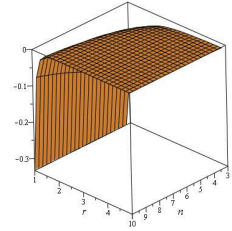
FIG. 3: Variation of energy density (ρ) with radial co-ordinate r and parameter n for the numerical values $\lambda = 10^4$, $q = 1$ and $r_0 = 1$.



4(A)



4(B)



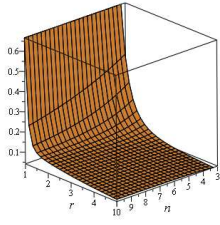
4(C)

FIG. 4: Variation of $\rho + p$ (4(A)), $\rho + 3p$ (4(B)), p (4(C)) with radial co-ordinate r and parameter n , have been plotted for obtained shape function(30) with redshift function $\phi(r) = \text{constant}$ when $\lambda = 10^4$, $q = 1$ and $r_0 = 1$.

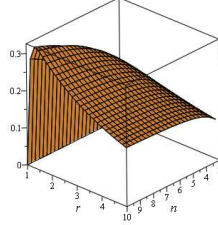
1. shape function $b(r) = \frac{r_0^n}{r^{n-1}}$, for some $n > 0$

For shape function (1), from the equation (11) we get the result,

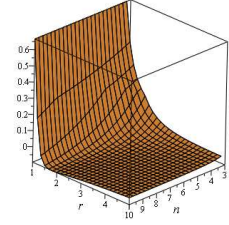
$$R = -2 \left(1 - \frac{r_0^n}{r^n} \right) \left[-\frac{\beta^2}{r^2} + \frac{\beta}{r^2} + \frac{(n-1)r_0^n}{r^{n+2} \left(1 - \frac{r_0^n}{r^n} \right)} - \frac{\beta \left\{ \frac{(1-n)r_0^n}{r^{n-1}} + \frac{3r_0^n}{r^{n-1}} - 4r \right\}}{2 r^3 \left(1 - \frac{r_0^n}{r^n} \right)} \right]. \quad (40)$$



5(A)

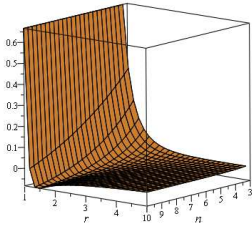


5(B)

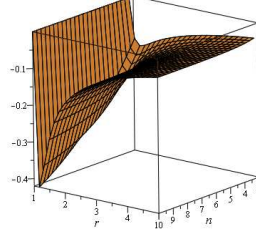


5(C)

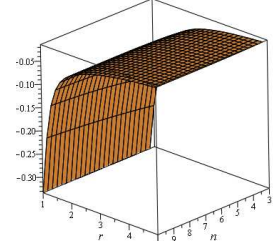
FIG. 5: Variation of $\rho + p$ (5(A)), $\rho + 3p$ (5(B)), $\rho - |p|$ (5(C)) with radial co-ordinate r and parameter n , have been plotted for obtained shape function(30) with redshift function $\phi(r) = \beta \ln\left(\frac{r}{r_0}\right)$ when $\lambda = 10^4$, $\beta = 0.5$, $q = 1$ and $r_0 = 1$.



6(A)

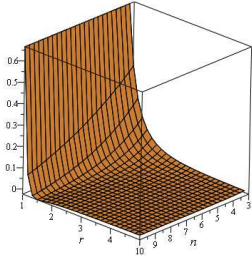


6(B)

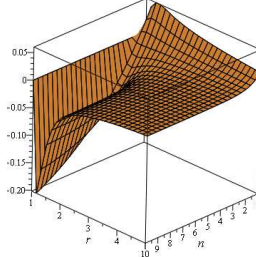


6(C)

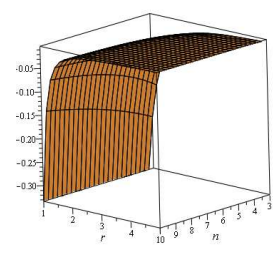
FIG. 6: Variation of $\rho + p$ (6(A)), $\rho + 3p$ (6(B)), p (6(C)) with radial co-ordinate r and parameter n , have been plotted for obtained shape function(30) with redshift function $\phi(r) = \frac{1}{r}$ when $\lambda = 10^4$, $q = 1$ and $r_0 = 1$.



7(A)



7(B)



7(C)

FIG. 7: Variation of $\rho + p$ (7(A)), $\rho + 3p$ (7(B)), p (7(C)) with radial co-ordinate r and parameter n , have been plotted for obtained shape function(30) with redshift function $\phi(r) = \ln\frac{\sqrt{\gamma^2+r^2}}{r}$ when $\lambda = 10^4$, $\gamma = 1$, $q = 1$ and $r_0 = 1$.

Therefore from (39) we obtain the expression of ρ for this model,

$$\rho = \frac{\lambda}{2(1 + \alpha^2\omega^2 + \omega^2 + \alpha\omega + 2\omega - 2\alpha\omega^2)} \left[(1 - \alpha\omega - 2\omega) + \left\{ (-1 + \alpha\omega + 2\omega)^2 \right. \right. \quad (41)$$

$$\left. \left. + \frac{(1 + \alpha^2\omega^2 + \omega^2 + \alpha\omega + 2\omega - 2\alpha\omega^2) \left(1 - \frac{r_0^n}{r^n}\right) \left\{ -\frac{\beta^2}{r^2} + \frac{\beta}{r^2} + \frac{(n-1)r_0^n}{r^{n+2} \left(1 - \frac{r_0^n}{r^n}\right)} - \frac{\beta}{2} \frac{\left\{ \frac{(1-n)r_0^n}{r^{n-1}} + \frac{3r_0^n}{r^{n-1}} - 4r \right\}}{r^3 \left(1 - \frac{r_0^n}{r^n}\right)} \right\}}{\pi\lambda} \right]^{1/2}.$$

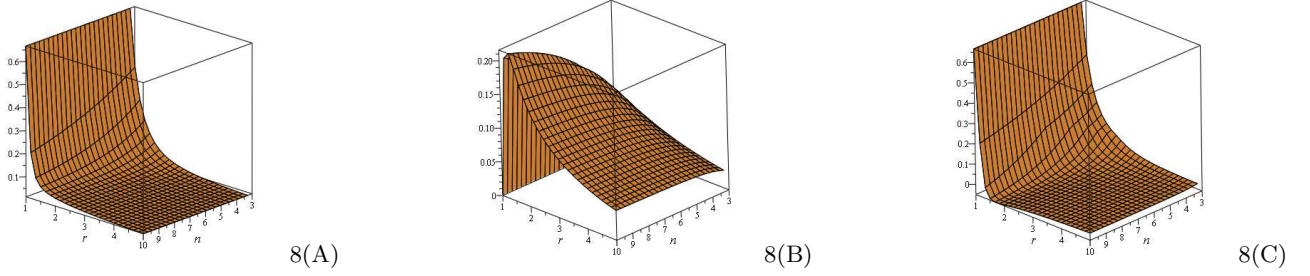


FIG. 8: Variation of $\rho + p$ (8(A)), $\rho + 3p$ (8(B)), $\rho - |p|$ (8(C)) with radial co-ordinate r and parameter n , have been plotted for obtained shape function(30) with redshift function $\phi(r) = e^{-\frac{r_0}{r}}$ when $\lambda = 10^4$, $q = 1$ and $r_0 = 1$.

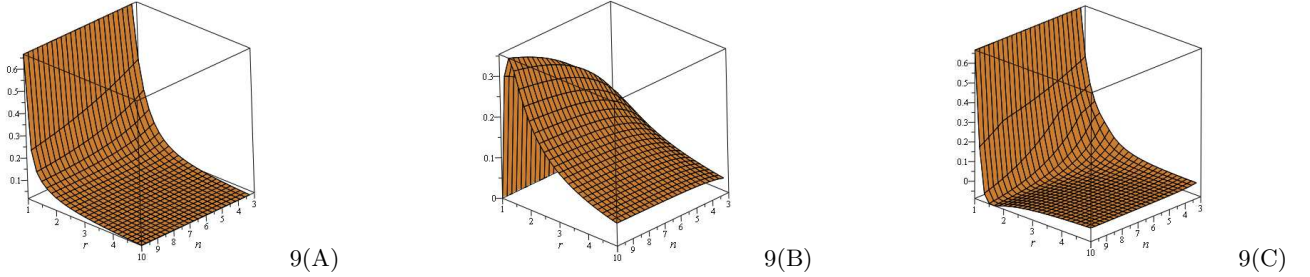


FIG. 9: Variation of $\rho + p$ (9(A)), $\rho + 3p$ (9(B)), $\rho - |p|$ (9(C)) with radial co-ordinate r and parameter n , have been plotted for obtained shape function(30) with redshift function $\phi(r) = e^{-\frac{r_0}{r} - \frac{r_0^2}{r^2}}$ when $\lambda = 10^4$, $q = 1$ and $r_0 = 1$.

$$2. \text{ shape function } b(r) = \frac{r}{1 + \ln(1 + r - r_0)}, \quad 0 < r_0 < 1$$

For shape function (2), from the equation (11) we get the result,

$$R = \frac{2\ln(1 + r - r_0)}{1 + \ln(1 + r - r_0)} \left[\frac{\beta}{r^2} - \frac{\beta^2}{r^2} + \frac{(1 - r_0) + (1 + r - r_0)\ln(1 + r - r_0)}{r(1 + r - r_0)(1 + \ln(1 + r - r_0))\ln(1 + r - r_0)} \right. \\ \left. + \frac{\beta(1 + \ln(1 + r - r_0))}{2r^2\ln(1 + r - r_0)} \left\{ \frac{(1 - r_0) + (1 + r - r_0)\ln(1 + r - r_0)}{(1 + \ln(1 + r - r_0))^2(1 + r - r_0)} + \frac{3}{1 + \ln(1 + r - r_0)} - 4 \right\} \right]. \quad (42)$$

Therefore from (39) we obtain the expression of ρ for this model,

$$\rho = \frac{\lambda}{2(1 + \alpha^2\omega^2 + \omega^2 + \alpha\omega + 2\omega - 2\alpha\omega^2)} \left[(1 - \alpha\omega - 2\omega) + \left\{ (-1 + \alpha\omega + \omega)^2 \right. \right. \\ \left. \left. - \frac{(1 + \alpha^2\omega^2 + \omega^2 + \alpha\omega + 2\omega - 2\alpha\omega^2)\ln(1 + r - r_0)}{\pi\lambda(1 + \ln(1 + r - r_0))} \left[\frac{\beta}{r^2} - \frac{\beta^2}{r^2} + \frac{(1 - r_0) + (1 + r - r_0)\ln(1 + r - r_0)}{r(1 + r - r_0)(1 + \ln(1 + r - r_0))\ln(1 + r - r_0)} \right. \right. \right. \\ \left. \left. \left. + \frac{\beta(1 + \ln(1 + r - r_0))}{2r^2\ln(1 + r - r_0)} \left\{ \frac{(1 - r_0) + (1 + r - r_0)\ln(1 + r - r_0)}{(1 + \ln(1 + r - r_0))^2(1 + r - r_0)} + \frac{3}{1 + \ln(1 + r - r_0)} - 4 \right\} \right] \right\}^{\frac{1}{2}} \right]. \quad (43)$$

$$3. \text{ shape function } b(r) = \frac{r}{1 + r - r_0}, \quad 0 < r_0 < 1$$

For shape function (3), from the equation (11) we get the result,

$$R = \frac{2(r - r_0)}{1 + r - r_0} \left[\frac{\beta}{r^2} - \frac{\beta^2}{r^2} + \frac{1 - r_0}{r^2(1 + r - r_0)} + \frac{\beta(1 + r - r_0)}{2r^2(r - r_0)} \left\{ \frac{1 - r_0}{(1 + r - r_0)^2} + \frac{3}{1 + r - r_0} - 4 \right\} \right]. \quad (44)$$

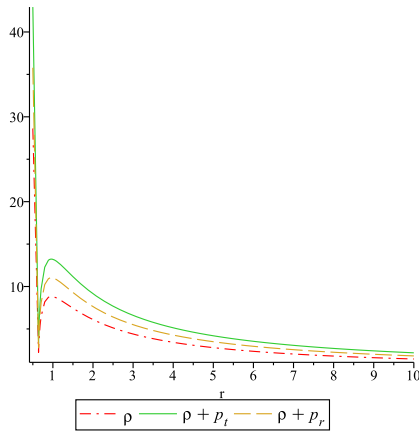


FIG.10(A)

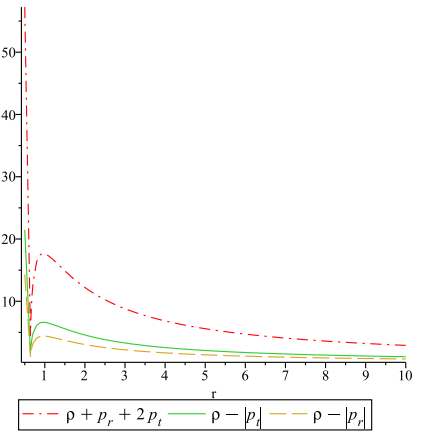


FIG.10(B)

FIG. 10: Behavior of ρ , $\rho + p_t$ and $\rho + p_r$ (FIG.10(A)) and $\rho + p_r + 2p_t$, $\rho - |p_t|$ and $\rho - |p_r|$ diagrams (FIG.10(B)) have been plotted for shape function (1) with non-zero tidal force against r when $\alpha = 2$, $\omega = 0.25$, $\lambda = 10^3$, $n = 0.9$, $\beta = -3$ and $r_0 = 0.5$.

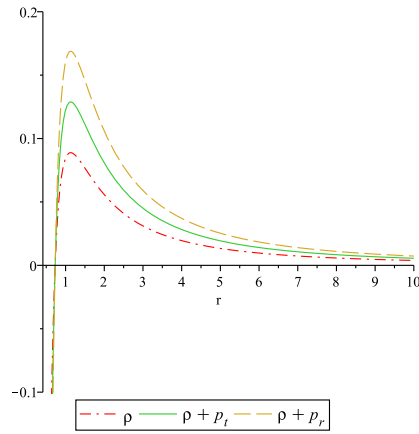


FIG.11(A)

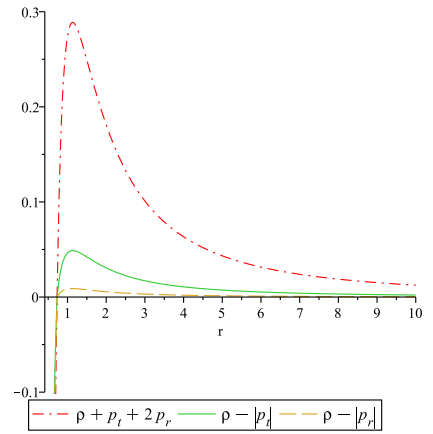


FIG.11(B)

FIG. 11: Behavior of ρ , $\rho + p_t$ and $\rho + p_r$ (FIG.11(A)) and $\rho + p_r + 2p_t$, $\rho - |p_t|$ and $\rho - |p_r|$ diagrams (FIG.11(B)) have been plotted for shape function(2) with non-zero tidal force against r when $\alpha = 2$, $\omega = 0.45$, $\lambda = 10^3$, $\beta = -3$ and $r_0 = 0.5$.

Therefore from (39) we obtain the expression of ρ for this model,

$$\begin{aligned} \rho = & \frac{\lambda}{2(1 + \alpha^2\omega^2 + \omega^2 + \alpha\omega + 2\omega - 2\alpha\omega^2)} \left[(1 - \alpha\omega - 2\omega) + \left\{ (-1 + \alpha\omega + 2\omega)^2 \right. \right. \\ & - \frac{(1 + \alpha^2\omega^2 + \omega^2 + \alpha\omega + 2\omega - 2\alpha\omega^2)(r - r_0)}{\pi\lambda(1 + r - r_0)} \left[\frac{\beta}{r^2} - \frac{\beta^2}{r^2} + \frac{1 - r_0}{r^2(1 + r - r_0)} \right. \\ & \left. \left. + \frac{\beta(1 + r - r_0)}{2r^2(r - r_0)} \left\{ \frac{1 - r_0}{(1 + r - r_0)^2} + \frac{3}{1 + r - r_0} - 4 \right\} \right] \right]^{\frac{1}{2}}. \end{aligned} \quad (45)$$

$$4. \text{ shape function } b(r) = r_0 \left\{ 1 + \gamma^2 \left(1 - \frac{r_0}{r} \right) \right\}, \text{ with } \gamma^2 \in (0, 1)$$

For shape function (4), from the equation (11) we get the result,

$$R = -\frac{2}{r} \left[\left(-\frac{\beta}{r^2} + \frac{\beta^2}{r^2} \right) \left\{ r - r_0 \left\{ 1 + \gamma^2 \left(1 - \frac{r_0}{r} \right) \right\} \right\} - \frac{\gamma^2 r_0^2}{r^3} - \frac{\beta}{2r^2} \left\{ \frac{\gamma^2 r_0^2}{r} + 3r_0 \left\{ 1 + \gamma^2 \left(1 - \frac{r_0}{r} \right) \right\} - 4r \right\} \right]. \quad (46)$$

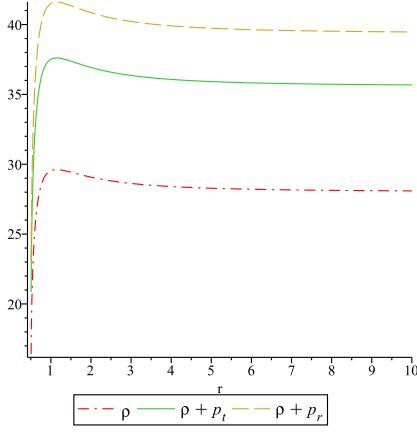


FIG.12(A)

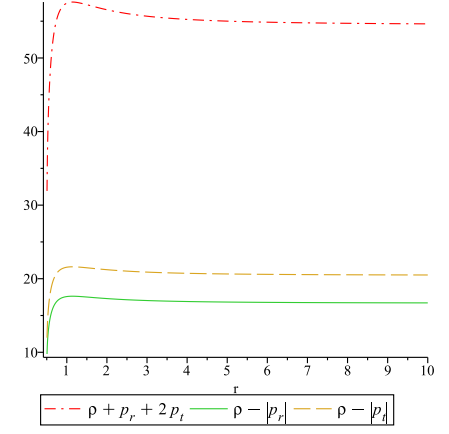


FIG.12(B)

FIG. 12: Behavior of ρ , $\rho + p_t$ and $\rho + p_r$ (FIG.12(A)) and $\rho + p_r + 2p_t$, $\rho - |p_t|$ and $\rho - |p_r|$ diagrams (FIG.12(B)) have been plotted for shape function(3) with non-zero tidal force against r for when $\alpha = 1.2$, $\omega = 0.27$, $\lambda = 10^3$, $\beta = -3$ and $r_0 = 0.5$.

Therefore from (39) we obtain the expression of ρ for this model,

$$\rho = \frac{\lambda}{2(1 + \alpha^2\omega^2 + \omega^2 + \alpha\omega + 2\omega - 2\alpha\omega^2)} \left[(1 - \alpha\omega - 2\omega) + \left\{ (-1 + \alpha\omega + 2\omega)^2 \right. \right. \\ \left. \left. + \frac{\gamma^2(1 + \alpha^2\omega^2 + \omega^2 + \alpha\omega + 2\omega - 2\alpha\omega^2)}{r\pi\lambda} \left[\left(-\frac{\beta}{r^2} + \frac{\beta^2}{r^2} \right) \left\{ r - r_0 \left\{ 1 + \gamma^2 \left(1 - \frac{r_0}{r} \right) \right\} \right\} - \frac{\gamma^2 r_0^2}{r^3} \right. \right. \right. \\ \left. \left. \left. - \frac{\beta}{2r^2} \left\{ \frac{\gamma^2 r_0^2}{r} + 3r_0 \left\{ 1 + \gamma^2 \left(1 - \frac{r_0}{r} \right) \right\} - 4r \right\} \right] \right\}^{\frac{1}{2}} \right]. \quad (47)$$

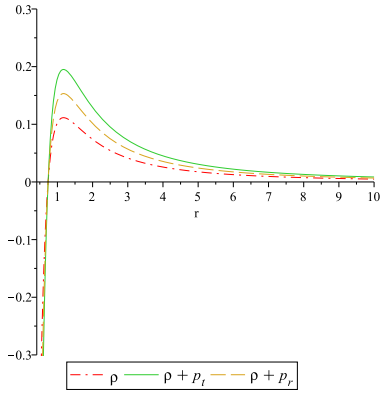


FIG.13(A)

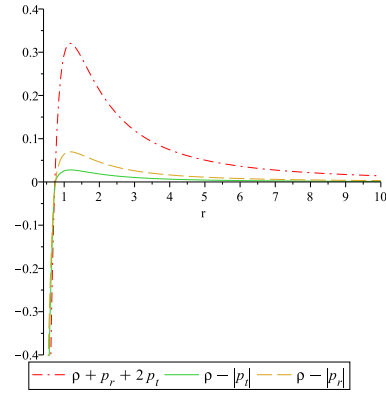


FIG.13(B)

FIG. 13: Behavior of ρ , $\rho + p_t$ and $\rho + p_r$ (FIG.13(A)) and $\rho + p_r + 2p_t$, $\rho - |p_t|$ and $\rho - |p_r|$ diagrams (FIG.13(B)) have been plotted for shape function(4) with non-zero tidal force against r when $\alpha = 0.5$, $\omega = 0.75$, $\lambda = 10^3$, $\gamma = 0.8$, $\beta = -3$ and $r_0 = 0.5$.

$$5. \quad \text{shape function } b(r) = r e^{\frac{2\sigma}{\delta}(r^\delta - r_0^\delta)} \text{ for some constant } \sigma < 0 \text{ and } \delta > 0$$

For shape function (5), from the equation (11) we get the result,

$$R = -\frac{2}{r^2} \left[(\beta^2 + \beta) - e^{\frac{2\sigma}{\delta}(r^\delta - r_0^\delta)} \{ \beta + \beta^2 + 1 + \sigma e^\delta (\beta + 2) \} \right]. \quad (48)$$

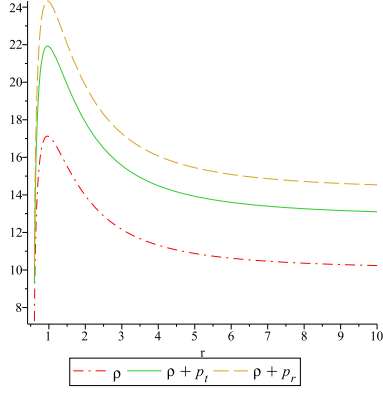


FIG.14(A)

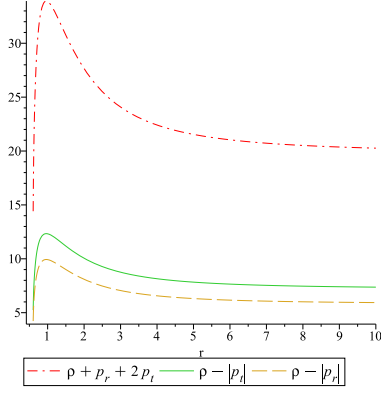
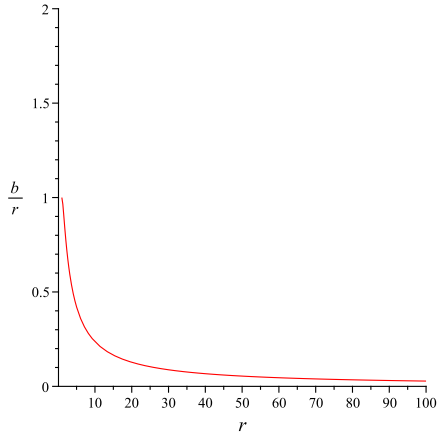
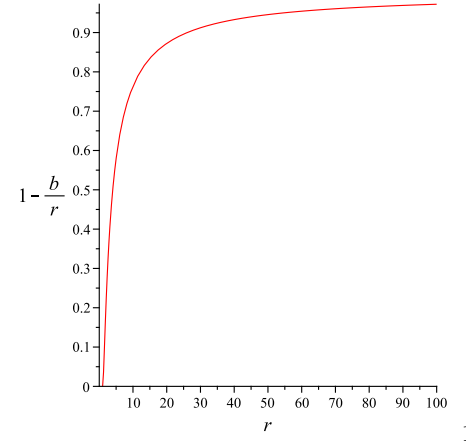


FIG.14(B)

FIG. 14: Behavior of ρ , $\rho + p_t$ and $\rho + p_r$ (FIG.14(A)) and $\rho + p_r + 2p_t$, $\rho - |p_t|$ and $\rho - |p_r|$ diagrams (FIG.14(B)) have been plotted for shape function(5) with non-zero tidal force against r when $\alpha = 1.5$, $\omega = 0.28$, $\lambda = 10^3$, $\sigma = -1$, $\delta = 1$, $\beta = -3$ and $r_0 = 0.5$.



15(A)



15(B)

FIG. 15: Behavior of $\frac{b(r)}{r}$ (15(A)), $1 - \frac{b(r)}{r}$ (15(B)) have been plotted for obtained shape function(30) against r when $n = 3.5$, $\lambda = 10^4$, $q = 1$ and $r_0 = 1$.

Therefore from (39) we obtain the expression of ρ for this model,

$$\rho = \frac{\lambda}{2(1 + \alpha^2\omega^2 + \omega^2 + \alpha\omega + 2\omega - 2\alpha\omega^2)} \left[(1 - \alpha\omega - 2\omega) + \sqrt{(-1 + \alpha\omega + 2\omega)^2 + \frac{(1 + \alpha^2\omega^2 + \omega^2 + \alpha\omega + 2\omega - 2\alpha\omega^2) \left\{ (\beta^2 + \beta) - e^{\frac{2\sigma}{8}(r^\delta - r_0^\delta)} \{ \beta + \beta^2 + 1 + \sigma e^\delta (\beta + 2) \} \right\}}{\pi\lambda r^2}} \right]. \quad (49)$$

VII. RESULTS AND DISCUSSION

A new shape function is obtained by considering $\rho = q \left(\frac{r}{r_0} \right)^{-n}$ and $\epsilon = 0$. Now the case $\epsilon = 0$ can be obtained when the space is conformally flat or in the vacuum space. Also it is observed that when $\epsilon = 0$ then the presence of exotic matter may depend upon the sign of σ_r . In other words if $\sigma_r < 0$ then the presence of exotic matter will be ensured (when ρ and λ both are positive)[35]. Wormhole solutions under many redshift functions so the figure of $\rho + p$ and $\rho - |p|$ will be identical for each case. All the energy conditions are examined in (FIG.3—FIG.9) for each wormhole

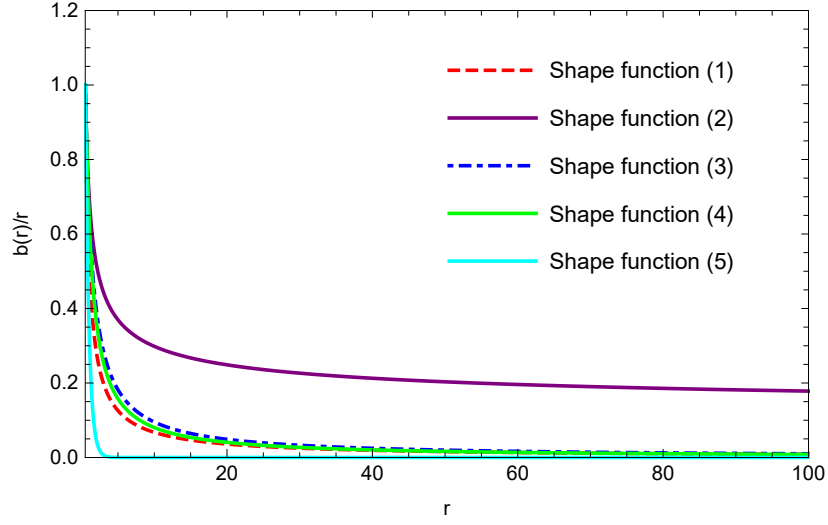


FIG. 16: Diagram of $\frac{b(r)}{r}$ vs. “ r ” for the five different shape functions when $n = 0.9, \gamma = 0.8, \sigma = -1, \delta = 1$ and $r_0 = 0.5$.

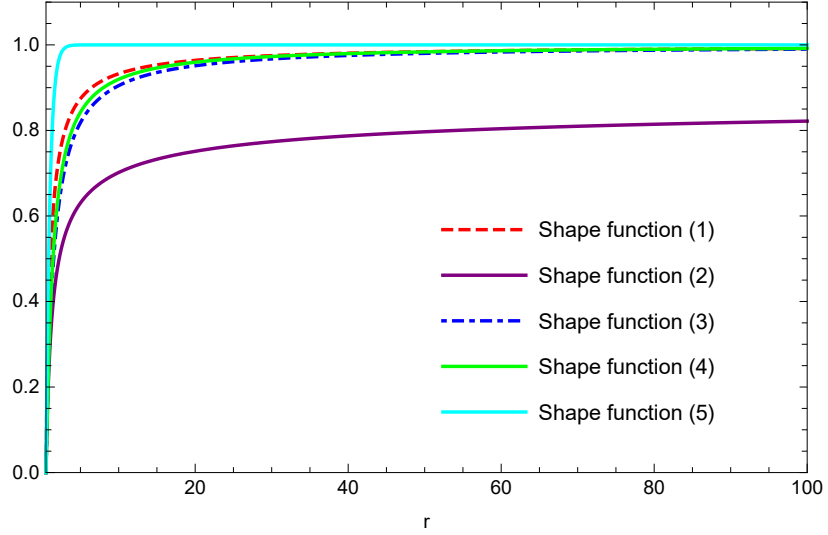


FIG. 17: Diagram of $1 - \frac{b(r)}{r}$ vs. “ r ” for the five different shape functions when $n = 0.9, \gamma = 0.8, \sigma = -1, \delta = 1$ and $r_0 = 0.5$.

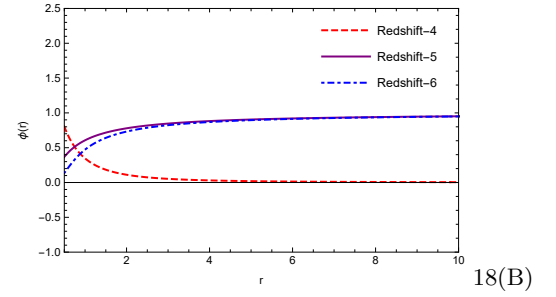
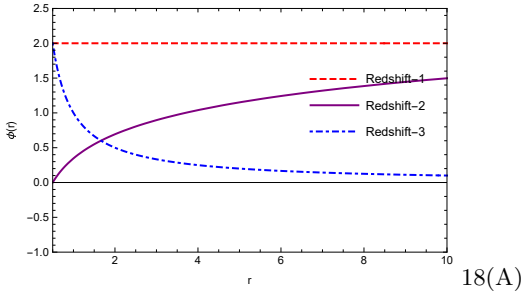


FIG. 18: Diagram of redshift functions $\phi(r) = \text{constant}$ (Redshift-1), $\phi(r) = \beta \ln\left(\frac{r}{r_0}\right)$ (Redshift-2), $\phi(r) = \frac{1}{r}$ (Redshift-3), $\phi(r) = \ln\frac{\sqrt{\gamma^2+r^2}}{r}$ (Redshift-4), $\phi(r) = e^{-\frac{r_0}{r}}$ (Redshift-5), $\phi(r) = e^{-\frac{r_0}{r} - \frac{r_0^2}{r^2}}$ (Redshift-6) when $\beta = 0.5, \gamma = 1$ and $r_0 = 0.5$.

TABLE I: Range of ‘ r ’ where energy conditions are satisfied for obtained shape function(30) when $n \in (3, 5)$ under isotropic scenario.

Redshift functions	NEC	WEC	SEC	DEC
$\phi(r) = \text{constant}$	$(r_0, 2)$	$(r_0, 2)$	\times	$(r_0, 2)$
$\phi(r) = \beta \ln\left(\frac{r}{r_0}\right)$	$(r_0, 5)$	$(r_0, 5)$	$(r_0, 5)$	$(r_0, 1.8)$
$\phi(r) = \frac{1}{r}$	$(r_0, 1.56)$	$(r_0, 1.56)$	\times	$(r_0, 1.56)$
$\phi(r) = \ln\left(\frac{\sqrt{\gamma^2+r^2}}{r}\right)$	$(r_0, 2)$	$(r_0, 2)$	\times	$(r_0, 2)$
$\phi(r) = e^{-\frac{r_0}{r}}$	$(r_0, 5)$	$(r_0, 5)$	$(r_0, 5)$	$(r_0, 2)$
$\phi(r) = e^{-\frac{r_0}{r} - \frac{r_0^2}{r^2}}$	$(r_0, 5)$	$(r_0, 5)$	$(r_0, 5)$	$(r_0, 1.75)$

solutions corresponding to mentioned redshift functions (for isotropic scenario). It is seen that for redshift functions $\phi(r) = \text{constant}$, $\phi(r) = \frac{1}{r}$, $\phi(r) = \ln\frac{\sqrt{\gamma^2+r^2}}{r}$ there exists a region for each cases where all energy conditions are satisfied except SEC for $n \in (3, 5)$. For the redshift functions $\phi(r) = \beta \ln\left(\frac{r}{r_0}\right)$, $\phi(r) = e^{-\frac{r_0}{r}}$ and $\phi(r) = e^{-\frac{r_0}{r} - \frac{r_0^2}{r^2}}$, all energy conditions are satisfied in a neighbourhood of the wormhole throat for $n \in (3, 5)$, which is clear from table I.

For anisotropic case, from the energy conditions, it can be observed from inequalities (12)–(15), if the relation between tangential and radial pressure is of the form $p_t = \omega\rho$ and $p_r = \alpha p_t$ ($\alpha \neq 1$), then all energy conditions will satisfy if $|\alpha\omega| \leq 1$, $|\omega| \leq 1$ and $\omega(\alpha + 2) \geq -1$ provided $\rho \geq 0$. Thus if $\alpha\omega, \omega \in (0, 1)$, then all energy conditions will be satisfied in the region where $\rho \geq 0$. Hence from the FIG.10–FIG.14, the region where $\rho \geq 0$, all energy conditions will satisfy.

For redshift function $\phi(r) = \beta \ln\left(\frac{r}{r_0}\right)$, the connecting asymptotic spaces by the wormhole are not flat in nature, in other all the considered cases connecting asymptotic spaces are flat except for the shape function (2)(from figures 15A, 16 and 18). From figures 15(B) and 17, we can conclude that all the wormholes corresponding to all shape functions throughout in this work are infinitely extendable[36].

Hence violation of NEC in the neighbourhood of wormhole throat which is necessary in Einstein gravity[14],[15],[17] to form a wormhole, is not necessary in brane-world gravity theory.

Acknowledgement

We thank Prof. Subenoy Chakraborty, Jadavpur University for the useful discussions about this work.

-
- [1] M. Cavaglia, *Int. J. Mod. Phys. A* **18**, 1843(2003).
[2] Roy Maartens, “Dark Energy from Brane World Gravity”, *astro-ph/060245*.
[3] P. Brax and C. V. Bruck, *Class. Quant. Grav.* **20**, R201(2003).
[4] L. Randall and R. Sundrum, *Phys. Rev. Lett.* **83**, 3370 (1999).
[5] R. Maartens, “ Geometry and Dynamics of the Brane World”, *Reference Frames and Gravitomagnetisms* 93-119(2001).
[6] N. Arkani-Hamed, S. Dimopoulos and G. Dvali, *Phys. Rev. D* **59**, 086004(1999).
[7] T. Shiromizu, K. Maeda and M. Sasaki, *Phys. Rev. D* **62**, 024012(2000).
[8] K. A. Bronnikov, Possible wormholes in a brane world, *Phys. Rev. D* **67**, 064027(2003).
[9] Francisco S. N. Lobo, General class of braneworld wormholes, *Phys. Rev. D* **75**, 064027(2007).
[10] F. Parsaei and N. Riazi, New wormhole solutions on the brane, *Phys. Rev. D* **91**, 024015(2015).
[11] L. Flamm, *Phys. Z* **17**, 448 (1916).
[12] A. Einstein and N. Rosen, The particle problem in the general theory of relativity, *Phys. Rev* **48**, 73(1935).
[13] Charles W. Misner and J. A. Wheeler, Classical physics as geometry, *Annals Of Physics* **2**, 525-603(1957).
[14] M. Visser, Lorentzian Wormholes: From Einstein to Hawking (*American Institute of Physics, New York*, 1996).
[15] N. Godani and Gauranga C. Samanta, Non-violation of energy conditions on wormholes modeling, *Mod. Phys. Lett. A* **34**, 1950226(2019).
[16] Gauranga C. Samanta and N. Godani, Wormhole modeling supported by non-exotic matter, *Mod. Phys. Lett. A* **34**, 1950224(2019).
[17] M. S. Morris, K. S. Thorne and U. Yurtsever, *Phys. Rev. Lett* **61**, 1446(1988).
[18] M. S. Morris and K. S. Throne, Wormholes in spacetime and their use for interstellar travel: a tool for teaching general relativity, *Am. J. Phys* **56**, 395(1988).

- [19] Roy Maartens, Brane-world gravity, *Living Reviews in Relativity* **7**, 7(2004).
- [20] Ayan Banerjee, P. H. R. S. Moraes, R. A. C. Correa and G. Ribeiro, Wormholes in Randall- Sundrum braneworld, *arXiv: 1904.10310*[gr-qc].
- [21] Deng Wang, Xin-He Meng, Traversable braneworld wormholes supported by astrophysical observations, *Frontiers of Physics* **13**, 139801(2018).
- [22] H. S. Tan, On Tidal Love Numbers of Braneworld Black Holes and Wormholes, *arXiv:2001.00403*[gr-qc].
- [23] F. Parsaei and N. Riazi, Evolving wormhole in the brane-world scenario, *arXiv: 2004.01750*[gr-qc].
- [24] K. C. Wong, T. Harko and K. S. Cheng, Inflating wormholes in the braneworld models, *Class. Quant. Gravity* **28**, 145023(2011).
- [25] Subenoy Chakraborty and Tanwi Bandyopadhyay, Wormhole and its analogue in brane world, *Astrophysics and Space science* **317**, 209-212(2008).
- [26] C. Molina and J. C. S. Neves, Black holes and wormholes in Ads branes, *Phys. Rev. D* **82**, 044029(2010).
- [27] C. Molina and J. C. S. Neves, Wormholes in de sitter branes, *Phys. Rev. D* **86**, 024015(2012).
- [28] M. La Camera, Wormhole solutions in the Randall-Sundrum scenario, *Phys. Lett. B* **573**, 27-32(2003).
- [29] Mauricio Cataldo, Luis Leimpi and Pablo Rodriguez, *Physics Letters B* **757**, 130-135 (2016).
- [30] Galin Gylchev, Petya Nedkova, Vassil Tinchev and Stoytcho Yazadjiev, On the shadow of rotating traversable wormholes, *Eur. Phys. J. C* **78**, 544(2018).
- [31] G. C. Samanta and N. Godani, Validation of energy conditions in Wormhole Geometry within viable $f(R)$ gravity, *arXiv: 04406v1*[gr-qc].
- [32] Francisco S. N. Lobo, “ Wormholes, Warp Drives and Energy Conditions”, *Springer*, 2017.
- [33] Daichi Tsuna, Ayko Ishii, Naota Kuriyama, Kazumi Kashiyaama and Toshikazu Shigeyama, Intermediate Luminosity Red Transients by Black Holes Born from Erupting Massive Stars, *The Astrophysical Journal Letters* **897**, 2(2020).
- [34] Pierre Christian and Abraham Loeb, Detecting Black Hole Occultations by Stars with Space Interferometric Telescopes, *The Astrophysical Journal Letters* **899**, 1(2020).
- [35] S. Nath and S. Chakraborty, *Astrophys Space Sci* **315**, 21-24(2008).
- [36] B.Ghosh et al., *Int. Jour. Mod. Phys. A* **36**, 2150046(2021).